

# Modeling Skin and Proximity Effects With Reduced Realizable $RL$ Circuits

Shizhong Mei and Yehea I. Ismail, *Member, IEEE*

**Abstract**—On-chip conductors such as clock- and power-distribution networks require accurately modeling skin and proximity effects. Furthermore, to incorporate skin and proximity effects in the existing generic simulation tools such as SPICE, simple-frequency independent-lumped element-circuit models are needed. A rule based  $RL$  circuit model is proposed in this paper that is realizable and predicts skin and proximity effects accurately in the frequency range of interest. With this circuit model, wires are characterized by a few parallel branches of resistors and inductors while proximity effect is captured by mutual inductance between inductors in different  $RL$  circuits.

**Index Terms**—Proximity effect,  $RLC$ , simulation, skin effect.

## I. INTRODUCTION

MULTIPLE metal layers are used for interconnect in high-performance VLSI circuits, with thicker layers on the top. To maintain low-clock skew and low electromigration, the clock- and power-distribution networks in the interconnect layers are made wide. Due to skin and proximity effects, resistance and inductance are frequency dependent. The trend is, the larger the cross section dimensions of the wire and the higher the frequency of interest, the more change in the resistance and inductance. With clock frequencies in the gigahertz range, it is necessary to use accurate skin and proximity effects models to capture the behavior of the clock- and power-distributions networks, especially the parts in the top layers.

Simulations [1] have shown that skin effect increases propagation delay substantially. Two time domain responses from that paper are plotted in Fig. 1 for an  $RLC$  tree of three  $RLC$  sections. One response is obtained by using the constant resistance and inductance while the other is obtained by using the exact frequency dependent resistance and inductance. The three extracted dc resistances are 25, 30, and 50  $\Omega$ , respectively. As shown in Fig. 1, ignoring skin effect underestimates the propagation delay by almost 20%. More simulations are provided in that paper for other wires. All the results show that the extra delay caused by skin effect cannot be ignored.

The fact that skin effect causes nonnegligible extra delay can be explained by looking into the frequency dependent behavior of resistances. Resistances increase with frequency due to skin effect. Fig. 2 shows the ratio of the frequency dependent resistance with respect to the dc value for two conductors of cross sections  $3 \mu\text{m} \times 40 \mu\text{m}$  and  $2 \mu\text{m} \times 40 \mu\text{m}$ , respectively. Circles

represent the values calculated from the volume filament model while solid curves represent those from the reduced  $RL$  circuits proposed in this paper. These results show that the proposed model works very well even for very wide wires that are harder to model accurately. For the  $2 \mu\text{m} \times 40 \mu\text{m}$  conductor, the 15% increase in the resistance occurs at 2.2 GHz. The clock frequency with the leading VLSI technology has already reached this number. With the rise time much less than the clock period, the main harmonic frequency component is much higher than 2.2 GHz, i.e., the increasing resistance of wide wires can affect the propagation delay significantly. Besides, an accurate skin effect model is critical for the analysis of signal integrity [2].

Skin effect is a well-known physical phenomenon. Several models [3]–[6] aim at finding the values of inductance and resistance as functions of frequency. Although these models are accurate, they are difficult to use with most available simulators [7]. Several other models aim at finding frequency independent lumped element circuits to replace the original frequency dependent elements. Among these models are the volume filament model [8], ladder model [9], and the compact circuit models [10]–[12]. All these models can be directly used in generic simulators such as SPICE. However, the volume filament model and the ladder model have large number of elements and are expensive in terms of computational time. The compact circuit model in [10] needs an iterative procedure to find the best circuit elements. Besides, since the model [10] uses semi-empirical formulae in calculating the circuit elements, its accuracy for conductors of arbitrary shapes is not guaranteed. The model in [11] involves empirical formulae that do not guarantee realizability in calculating circuit elements, i.e., this model does not always produce positive resistances and inductances. Although the model in [12] gives accurate results for several important interconnect structures, its accuracy for a general interconnect wire is not demonstrated.

The method described here starts with the volume filament model and proceeds to produce an equivalent  $RL$  circuit for any wire. The equivalent  $RL$  circuit, which captures skin effect in a wire, contains only a few resistors and inductors in parallel. Rather than using any empirical formula as, e.g., [10] and [11], the proposed method here only uses geometrical dimensions of wires and produces the accurate equivalent  $RL$  circuit efficiently through a systematic mathematical technique. When proximity effect between wires becomes nonnegligible, it is assumed that each wire is still represented by its equivalent  $RL$  circuit. However, to capture proximity effect, mutual inductance elements are added between coupled wires.

The rest of the paper is organized as follows. The approach to obtain reduced and decoupled  $RL$  circuits is explained in Sec-

Manuscript received February 18, 2003; revised July 28, 2003.

The authors are with the Electrical and Computer Engineering Department, Northwestern University, Evanston, IL 60208 USA (e-mail:meisz@ece.northwestern.edu).

Digital Object Identifier 10.1109/TVLSI.2004.825863

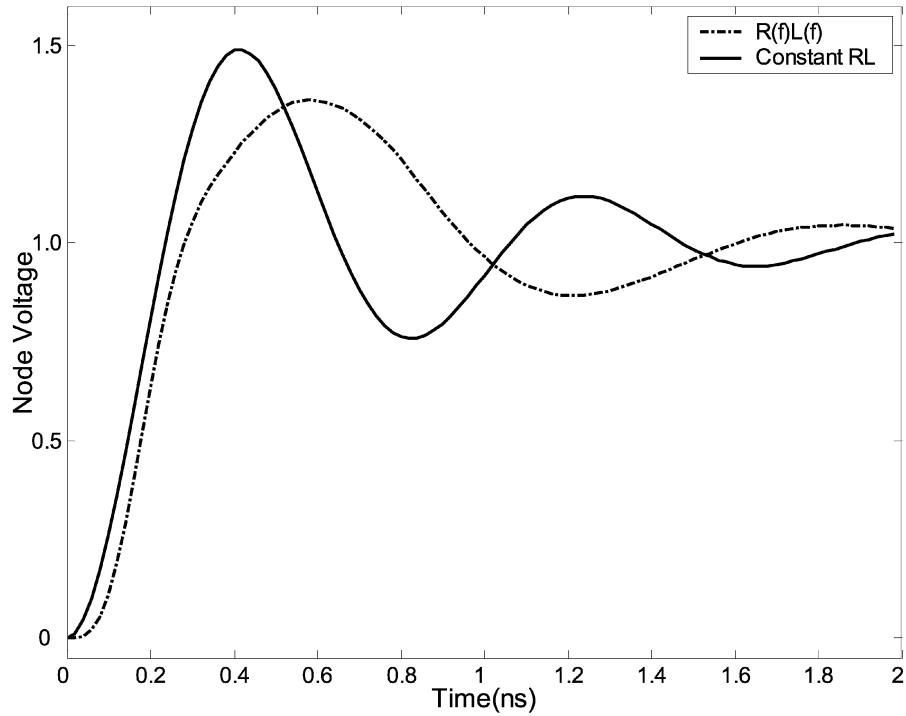


Fig. 1. Time-domain responses.

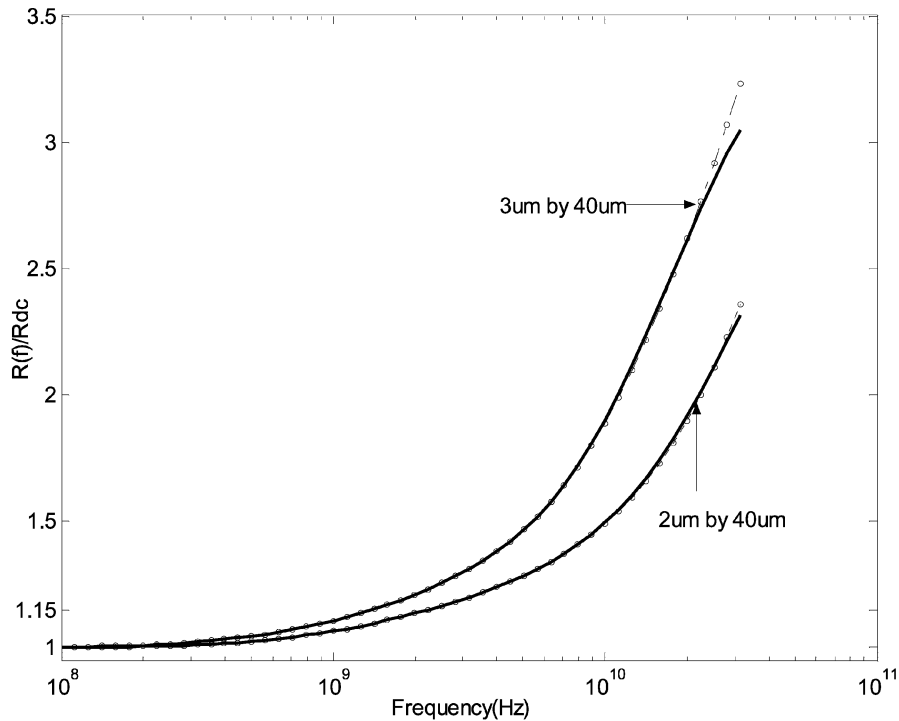


Fig. 2. Increasing resistances with frequency due to skin effect.

tion II. Section III explains the rule to determine mutual inductance between reduced  $RL$  circuits to capture the proximity effect between wires. Section IV compares the frequency-dependent resistance and inductance calculated from the reduced and coupled  $RL$  circuits and those from the original circuits when skin and proximity effects are prominent. Conclusions are given in Section V.

## II. SKIN EFFECT MODEL

At dc, the current in a conductor is evenly distributed over the cross section. Skin effect occurs when alternating current flows through a conductor. The alternating current induces a time varying magnetic field, which in turn induces electrical field and causes an uneven distribution of current over the cross

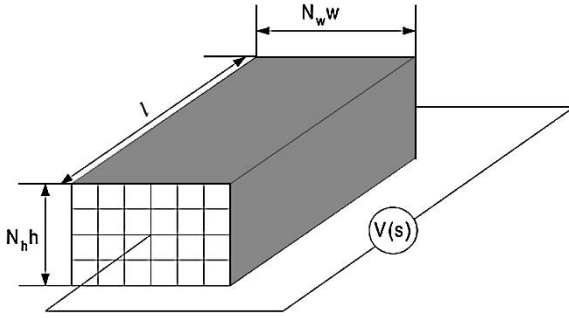
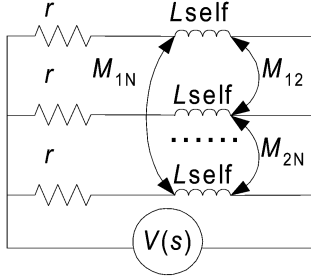

 Fig. 3. A rectangular conductor driven by voltage  $V(s)$ .


Fig. 4. The original circuit of an isolated wire.

section of the conductor. The electrical current tends to crowd toward the surface of the conductor, leading to an increase in the resistance and a decrease in the internal inductance.

If the cross section of the conductor is divided into much smaller sections, then the current distribution in each filament can be regarded as uniform. The frequency dependent resistance and inductance can be obtained by solving the currents in the inductively coupled  $RL$  branches, which is the main idea of the volume filament model.

Fig. 3 shows a rectangular conducting wire driven by any voltage  $V(s)$ . To apply the volume filament model, the cross section is divided into  $N_w \times N_h$  identical filaments with width  $w$ , height  $h$ , and length  $l$  for each filament. Assume  $N_w$  and  $N_h$  are large enough, so that the current density in each filament is essentially uniform. Denoting  $\sigma$  the conductivity of the wire, the resistance of each filament is given by

$$r = \frac{l}{\sigma w h}. \quad (1)$$

The self-inductance for each filament is [13]

$$L_{\text{self}} = 0.2l \left[ \ln \left( \frac{2l}{w+h} \right) + 0.5 + 0.2235 \frac{w+h}{l} \right] \mu\text{H}. \quad (2)$$

Denoting  $d_{ij}$  the distance between the center axes of the  $i$ th and the  $j$ th filaments ( $i \neq j$ ), the mutual inductance between the two filaments is [14]

$$M_{ij} = 0.2l \left[ \ln \left( \frac{l}{d_{ij}} + \sqrt{1 + \frac{l^2}{d_{ij}^2}} \right) - \sqrt{1 + \frac{d_{ij}^2}{l^2}} + \frac{d_{ij}}{l} \right] \mu\text{H}. \quad (3)$$

With these parameters, the conductor in Fig. 3 is equivalent to the circuit in Fig. 4 where  $N = N_w N_h$ .

To guarantee an almost even distribution of current in each filament, the dimension of the filament  $w$  and  $h$  are selected to be smaller than the skin depth at the highest frequency of interest. This criterion means large number of filaments, e.g., 20, needed to replace wide conductors with significant skin effect. Non-uniform division of the conductor cross sectional area with fine division near the surface and coarse division away from the surface can reduce the total number of divisions. However, direct application of this volume filament model to simulate large interconnect circuits with significant skin effect is still formidable. A more efficient way of using the volume filament model is to reduce the original coupled  $RL$  circuit to a circuit of a few, e.g., 3, *decoupled*  $RL$  branches in parallel.

The voltage drop on any  $RL$  branch in Fig. 4 is  $V(s)$ . According to Ohm's law, the voltage drop  $V(s)$  equals the current in each  $RL$  branch times the impedance of each branch, which in matrix form is given by

$$V(s) \begin{bmatrix} 1 \\ 1 \\ \vdots \\ 1 \end{bmatrix} = r \begin{bmatrix} i_1 \\ i_2 \\ \vdots \\ i_N \end{bmatrix} + s \begin{bmatrix} L_{\text{self}} & M_{12} & \cdots & M_{1N} \\ M_{21} & L_{\text{self}} & \cdots & M_{2N} \\ \vdots & \vdots & \ddots & \vdots \\ M_{N1} & M_{N2} & \cdots & L_{\text{self}} \end{bmatrix} \begin{bmatrix} i_1 \\ i_2 \\ \vdots \\ i_N \end{bmatrix} \quad (4)$$

where  $i_1, i_2, \dots$ , and  $i_N$  are the currents in each  $RL$  branch. For simplicity, four symbols  $\mathbf{1}_N, \mathbf{E}_N, \mathbf{I}, \mathbf{L}$  are introduced to describe an  $N \times 1$  vector of all ones, an  $N \times N$  identity matrix, the current vector in (4), and the self/mutual inductance matrix in (4), respectively. In terms of  $\mathbf{1}_N, \mathbf{E}_N, \mathbf{I}$ , and  $\mathbf{L}$ , (4) can be rewritten as

$$V(s)\mathbf{1}_N = r\mathbf{E}_N\mathbf{I} + s\mathbf{L}\mathbf{I}. \quad (5)$$

The symmetric matrix  $\mathbf{L}$  is positive semidefinite [15], meaning that all the eigenvalues of  $\mathbf{L}$  are nonnegative real numbers. Because  $\mathbf{L}$  is real and symmetrical, there always exist normal and orthogonal matrices to diagonalize it. Denoting  $\mathbf{Q}$  as any normal and orthogonal matrix that diagonalizes  $\mathbf{L}$  and  $\mathbf{L}_{\text{Diag}}$  as the diagonal matrix, the following relations hold:

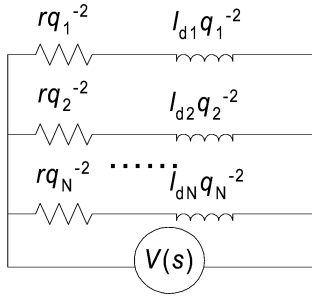
$$\mathbf{L}_{\text{Diag}} = \mathbf{Q}^T \mathbf{L} \mathbf{Q} = \begin{bmatrix} l_{d1} & 0 & \cdots & 0 \\ 0 & l_{d2} & \cdots & 0 \\ \vdots & \vdots & \ddots & \vdots \\ 0 & 0 & \cdots & l_{dN} \end{bmatrix} \quad \text{and} \\ \mathbf{Q}\mathbf{Q}^T = \mathbf{Q}^T\mathbf{Q} = \mathbf{E}_N \quad (6)$$

where  $l_{d1}, l_{d2}, \dots$ , and  $l_{dN}$  are nonnegative real eigenvalues.

Given the voltage  $V(s)$ , the total current in all  $RL$  branches should be computed to obtain the total impedance of the  $RL$  circuit in Fig. 4. By using (5) and (6), the total current  $I_t$  is calculated as

$$I_t = \mathbf{1}_N^T \mathbf{Q} (r\mathbf{E}_N + s\mathbf{L}_{\text{Diag}})^{-1} \mathbf{Q}^T \mathbf{1}_N V(s). \quad (7)$$

The product  $\mathbf{1}_N^T \mathbf{Q}$  and its transpose  $\mathbf{Q}^T \mathbf{1}_N$  are a row and a column vectors respectively. If the  $i$ th element of  $\mathbf{1}_N^T \mathbf{Q}$  or

Fig. 5. Equivalent  $RL$  circuit.

$\mathbf{Q}^T \mathbf{1}_N$  is represented by the symbol  $q_i$ , and the  $ij$ th element of  $(r\mathbf{E}_N + s\mathbf{L}_{\text{Diag}})^{-1}$  is represented by the symbol  $y_{ij}$ , then  $I_t$  in (7) can be re-expressed as

$$I_t = V(s) \sum_{i,j=1}^N q_i y_{ij} q_j. \quad (8)$$

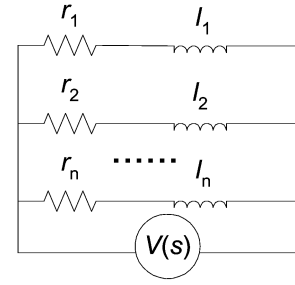
Since matrix  $(r\mathbf{E}_N + s\mathbf{L}_{\text{Diag}})^{-1}$  is diagonal, among  $y_{ij}$ 's only  $y_{ii}$ 's are nonzero and equal to  $1/(r + sl_{di})$ . So the right hand side of (8) further reduces to  $V(s) \sum_{i=1}^N q_i^2 / (r + sl_{di})$  and the total conductance  $Y_t$  becomes

$$Y_t = \sum_{i=1}^N \frac{q_i^2}{r + sl_{di}}. \quad (9)$$

Equation (9) implies that the circuit in Fig. 4 can *always* be replaced by  $N$  decoupled  $RL$  branches with resistance and inductance equal to  $r/q_i^2$  and  $l_{di}/q_i^2$  respectively, as shown in Fig. 5, i.e., the number of branches equals the number of filaments. Because all  $r/q_i^2$  and  $l_{di}/q_i^2$  are positive, the decoupling process guarantees realizability.

Branches of resistance  $r/q_i^2$  and inductance  $l_{di}/q_i^2$  can be grouped to reduce the total branch number. They can be grouped such that the branches in any group are within one order of magnitude from each other. The elements in each group can be combined to get a branch with the new resistance equal to the total parallel resistance and the new inductance equal to the total parallel inductance. The logic behind this reduction is that the resistance of the branch matches the low-frequency impedance of the group while the inductance of the branch matches the impedance of the group at high frequency. In the intermediate frequency range, the impedance of the branch more or less matches the impedance of the group. To further reduce the size of the  $RL$  circuit, the conductance of each equivalent  $RL$  branch at the highest frequency of interest is calculated and those  $RL$  branches whose conductance contribute a little to the overall conductance, e.g., less than 1%, are removed from the  $RL$  circuit.

Finding  $\mathbf{Q}$  directly is computationally expensive. However, the reduced  $RL$  circuit only contains a few dominant branches. Hence, it is unnecessary to get all the decoupled  $RL$  branches and reduce the circuit afterwards. A much faster approach is to directly determine these dominant branches. Since the total conductance of the reduced  $RL$  circuit matches that of the original circuit accurately (simulated results will be shown in Section IV), the difference in the leading coefficients of both con-

Fig. 6. Reduced  $RL$  circuit.

ductances should be negligible when both conductances are expanded in powers of  $s$ . The total conductance  $Y_t$  of the original circuit can be obtained directly from (5) as

$$Y_t = \mathbf{1}_N^T (r\mathbf{E}_N + s\mathbf{L})^{-1} \mathbf{1}_N \quad (10)$$

or expanded in powers of  $s$  as

$$Y_t = \sum_{i=0}^{\infty} y_i s^i \quad (11)$$

where  $y_i = \mathbf{1}_N^T (-\mathbf{L})^i \mathbf{1}_N r^{-(i+1)}$ . Without loss of generality, suppose that the conductance of  $n$  new  $RL$  branches in parallel approximates  $Y_t$  accurately in the frequency range of interest. Denote the new branches of resistance and inductance as  $r_1, l_1, r_2, l_2, \dots$  and  $r_n, l_n$ , respectively, and the total conductance as  $Y_{ta}$ . The expansion of  $Y_{ta}$  in powers of  $s$  is given by

$$Y_{ta} = \sum_{i=0}^{\infty} y_{ai} s^i \quad (12)$$

where  $y_{ai} = \sum_{j=1}^n (1/r_j) (-l_j/r_j)^i$ . A much faster way of determining values of  $r_1, l_1, r_2, l_2, \dots$  and  $r_n, l_n$  is to equate the leading  $4n$  coefficients  $y_{ai}$  and  $y_i$  ( $i = 1, 2, \dots, 2n$ ), respectively. With this process, circuits to describe wires with prominent skin effect reduce from large size as shown in Fig. 4 or Fig. 5 to much smaller size as illustrated in Fig. 6.

### III. SKIN AND PROXIMITY EFFECTS MODEL

The simplification process explained in the previous section ignores proximity effect completely. However, proximity effect can be prominent for very close wires. When this effect is significant, measures must be taken to handle it while keeping the simplicity of the equivalent circuits.

Proximity effect originates from inductive coupling between wires. As with inductive coupling, proximity effect diminishes as the distance between wires increases. In the extreme situation where wires are far apart, both proximity effect and inductive coupling between wires become negligible and each wire is accurately described by the reduced and decoupled  $RL$  circuit. It is reasonable to ascribe proximity effect between wires to the mutual inductance between inductors in different  $RL$  circuits. More specifically, each wire is described by its reduced and decoupled  $RL$  circuit that captures skin effect. To capture proximity effect, mutual inductance is added to inductors in different  $RL$  circuits. The rest of this section will explain how to calculate the mutual inductance parameters and to which pair of inductors to add them.

TABLE I  
 RESISTANCE AND INDUCTANCE VALUES IN THE REDUCED  $RL$  CIRCUITS

Conductors of $1\mu\text{m}$ thick and $20\mu\text{m}$ long				
# of $RL$ branches	Element	Conductor Width ( $\mu\text{m}$ )		
		2	5	10
2	Resistance ( $\Omega$ )	$r_1 = 121.72$ $r_2 = 0.286$	$r_1 = 23.51$ $r_2 = 0.115$	$r_1 = 7.17$ $r_2 = 0.058$
	Inductance (pH)	$l_1 = 267$ $l_2 = 12.6$	$l_1 = 201$ $l_2 = 10$	$l_1 = 142$ $l_2 = 7.9$
3	Resistance ( $\Omega$ )	Not needed	$r_1 = 144.59$ $r_2 = 27.95$ $r_3 = 0.115$	$r_1 = 43.4$ $r_2 = 8.5$ $r_3 = 0.058$
	Inductance (pH)		$l_1 = 341$ $l_2 = 279$ $l_3 = 10$	$l_1 = 280$ $l_2 = 197$ $l_3 = 7.9$

The low-frequency resistance and inductance are constant for any given wire. That means only one  $RL$  branch is essentially conducting at low frequency. Other branches start to conduct at high frequency, changing the total current and the total impedance with frequency. This conclusion can also be drawn from the simulation results in Table I that lists the resistances and inductances of the reduced  $RL$  circuits of three different wires. It is clearly shown in Table I that in each  $RL$  circuit, one branch has much smaller  $R$  and  $L$  values than the rest branches. Therefore, one mutual inductance between the two conducting branches at low frequency will suffice to capture the low-frequency proximity effect between any two wires. To capture high frequency proximity effect, mutual inductance should be assigned to other pairs of inductors with inductors in the same pair belonging to different wires. Since in each wire the  $RL$  branch that conducts at low frequency solely has by far the smallest impedance and the largest branch current, it is reasonable to neglect inductive coupling between inductors in different wires that do not conduct at low frequency. After this approximation, the total number of mutual inductances between two reduced  $RL$  circuits is roughly the total number of  $RL$  branches in both circuits. To give a quantitative description of the coupling, consider two reduced  $RL$  circuits with branch numbers  $n_1$  and  $n_2$ , respectively. According to the approximation, all  $n_1$  inductors in circuit one couple to the same inductor that has the smallest inductance in circuit two. On the other hand, all  $n_2$  inductors in circuit two couple to the same inductor that has the smallest inductance in circuit one. In total, there are  $n_1 + n_2 - 1$  mutual inductances between the two  $RL$  circuits. To further simplify the situation, assume all the  $n_1 + n_2 - 2$  mutual inductances other than that existing between the two smallest inductors are the same. So, only two mutual inductance parameters are used to capture the proximity effect between two wires in the frequency range of interest, as illustrated in Fig. 8.

For purpose of quantitative analysis of how to calculate the two mutual inductance parameters, consider two original  $RL$  circuits shown in Fig. 7 that describe the filament resistance and inductance in any two wires. Given any two wires, the

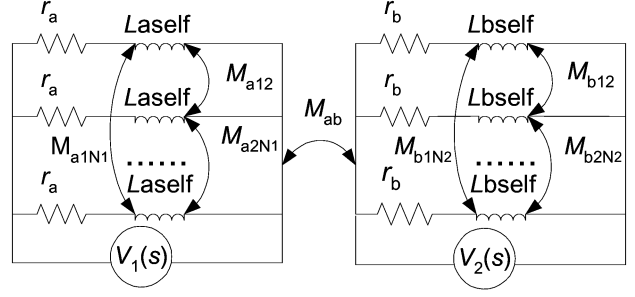


Fig. 7. The original circuit of two coupled wires.

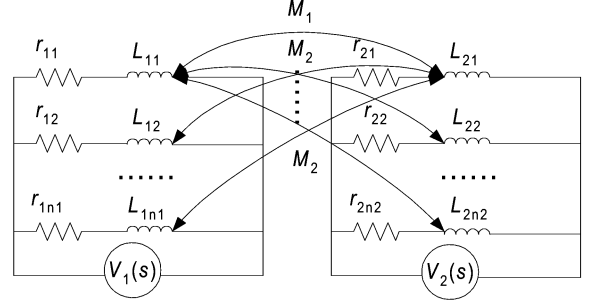


Fig. 8. The reduced circuit of two coupled wires.

filaments in one wire can be made identical but they may be different from those in the other wire due to inequality in length. To accommodate this possible difference, filament resistance, filament inductance, and mutual inductance between filaments in wire one are indicated by symbols  $r_a$ ,  $L_{a\text{self}}$ , and  $M_{aij}$  ( $i \neq j, 1 \leq i, j \leq N_1$ ), respectively while their counterparts in wire two are indicated by different symbols  $r_b$ ,  $L_{b\text{self}}$ , and  $M_{bij}$  ( $i \neq j, 1 \leq i, j \leq N_2$ ). Similar to matrices in (5),  $\mathbf{1}_{N_1}$  ( $\mathbf{0}_{N_1}$ ),  $\mathbf{1}_{N_2}$  ( $\mathbf{0}_{N_2}$ ),  $\mathbf{E}_{N_1}$  ( $\mathbf{E}_{N_2}$ ),  $\mathbf{I}_1$  ( $\mathbf{I}_2$ ), and  $\mathbf{L}_1$  ( $\mathbf{L}_2$ ) are introduced to refer to an  $N_1 \times 1$  vector of all ones(zeros), an  $N_2 \times 1$  vector of all ones(zeros), an  $N_1 \times N_1$  ( $N_2 \times N_2$ ) identity matrix, the current vector in wire one(two), and the self/mutual inductance matrix in wire one(two), respectively. Besides, an  $N_1 \times N_2$  matrix  $\mathbf{M}_{ab}$  describes the mutual inductance between filaments in wire one and filaments in wire two. Similar to (5), the voltage current relation in the two wires are obtained as

$$\begin{bmatrix} \mathbf{I}_1 \\ \mathbf{I}_2 \end{bmatrix} = \begin{bmatrix} r_a \mathbf{E}_{N_1} + s\mathbf{L}_a & s\mathbf{M}_{ab} \\ s\mathbf{M}_{ab}^T & r_b \mathbf{E}_{N_2} + s\mathbf{L}_b \end{bmatrix}^{-1} \begin{bmatrix} V_1(s)\mathbf{1}_{N_1} \\ V_2(s)\mathbf{1}_{N_2} \end{bmatrix}. \quad (13)$$

The total currents in wire one and wire two are easily calculated as

$$\begin{aligned} \mathbf{I}_{1t} &= [\mathbf{1}_{N_1} \mathbf{0}_{N_2}]^T \begin{bmatrix} r_a \mathbf{E}_{N_1} + s\mathbf{L}_a & s\mathbf{M}_{ab} \\ s\mathbf{M}_{ab}^T & r_b \mathbf{E}_{N_2} + s\mathbf{L}_b \end{bmatrix}^{-1} \\ &\quad \times \begin{bmatrix} V_1(s)\mathbf{1}_{N_1} \\ V_2(s)\mathbf{1}_{N_2} \end{bmatrix} \end{aligned} \quad (14)$$

$$\begin{aligned} \mathbf{I}_{2t} &= [\mathbf{0}_{N_1} \mathbf{1}_{N_2}]^T \begin{bmatrix} r_a \mathbf{E}_{N_1} + s\mathbf{L}_a & s\mathbf{M}_{ab} \\ s\mathbf{M}_{ab}^T & r_b \mathbf{E}_{N_2} + s\mathbf{L}_b \end{bmatrix}^{-1} \\ &\quad \times \begin{bmatrix} V_1(s)\mathbf{1}_{N_1} \\ V_2(s)\mathbf{1}_{N_2} \end{bmatrix} \end{aligned} \quad (15)$$

respectively.

Fig. 8 shows the reduced  $RL$  circuit to capture both skin and proximity effects of the two wires under consideration. Very similar to (14) and (15), the total currents in the reduced circuit one and two are

$$I'_{1t} = [\mathbf{1}_{n_1} \mathbf{0}_{n_2}]^T \begin{bmatrix} \mathbf{R}_1 + s\mathbf{L}_1 & s\mathbf{M} \\ s\mathbf{M}^T & \mathbf{R}_2 + s\mathbf{L}_2 \end{bmatrix}^{-1} \times \begin{bmatrix} V_1(s)\mathbf{1}_{n_1} \\ V_2(s)\mathbf{1}_{n_2} \end{bmatrix} \quad (16)$$

$$I'_{2t} = [\mathbf{0}_{n_1} \mathbf{1}_{n_2}]^T \begin{bmatrix} \mathbf{R}_1 + s\mathbf{L}_1 & s\mathbf{M} \\ s\mathbf{M}^T & \mathbf{R}_2 + s\mathbf{L}_2 \end{bmatrix}^{-1} \times \begin{bmatrix} V_1(s)\mathbf{1}_{n_1} \\ V_2(s)\mathbf{1}_{n_2} \end{bmatrix} \quad (17)$$

respectively.

To capture skin and proximity effects exactly, (16) should be equivalent to (14) and (17) should be equivalent to (15). However, this requirement is too stringent. Practically a much more relaxed condition can be used that only requires the second and third coefficients in  $I'_{1t}$  and  $I'_{2t}$  when expanded in powers of  $s$  equal to those in  $I_{1t}$  and  $I_{2t}$ , respectively (the first coefficients are not controlled by the mutual inductance parameters and the accurate reduction process explained in Section II guarantees the closeness of the first coefficients). Since the voltage sources  $V_1(s)$  and  $V_2(s)$  can take arbitrary values, the relaxed condition requires selecting two mutual inductance parameters to satisfy eight equations. Because of the symmetry of the resistance and inductance matrices in (14)–(17), the number of equations reduces to four. Mathematically, there may be no solution to satisfy the four equations simultaneously. However, if there exist two mutual inductance parameters such that the four equations are satisfied within minor errors, then the second and third coefficients in

$$[\mathbf{1}_{n_1} \mathbf{1}_{n_2}]^T \begin{bmatrix} \mathbf{R}_1 + s\mathbf{L}_1 & s\mathbf{M} \\ s\mathbf{M}^T & \mathbf{R}_2 + s\mathbf{L}_2 \end{bmatrix}^{-1} \begin{bmatrix} \mathbf{1}_{n_1} \\ \mathbf{1}_{n_2} \end{bmatrix}$$

when expanded in powers of  $s$  match those in

$$[\mathbf{1}_{N_1} \mathbf{1}_{N_2}]^T \begin{bmatrix} r_a \mathbf{E}_{N_1} + s\mathbf{L}_a & s\mathbf{M}_{ab} \\ s\mathbf{M}_{ab}^T & r_b \mathbf{E}_{N_2} + s\mathbf{L}_b \end{bmatrix}^{-1} \begin{bmatrix} \mathbf{1}_{N_1} \\ \mathbf{1}_{N_2} \end{bmatrix}$$

when expanded in powers of  $s$ , respectively, within minor errors. An example provided in Section IV indicates the existence of the two parameters that satisfy the four equations with high accuracy. So the second and third coefficients in

$$[\mathbf{1}_{n_1} \mathbf{1}_{n_2}]^T \begin{bmatrix} \mathbf{R}_1 + s\mathbf{L}_1 & s\mathbf{M} \\ s\mathbf{M}^T & \mathbf{R}_2 + s\mathbf{L}_2 \end{bmatrix}^{-1} \begin{bmatrix} \mathbf{1}_{n_1} \\ \mathbf{1}_{n_2} \end{bmatrix}$$

are matched with those in

$$[\mathbf{1}_{N_1} \mathbf{1}_{N_2}]^T \begin{bmatrix} r_a \mathbf{E}_{N_1} + s\mathbf{L}_a & s\mathbf{M}_{ab} \\ s\mathbf{M}_{ab}^T & r_b \mathbf{E}_{N_2} + s\mathbf{L}_b \end{bmatrix}^{-1} \begin{bmatrix} \mathbf{1}_{N_1} \\ \mathbf{1}_{N_2} \end{bmatrix}$$

respectively, in determining the two mutual inductance parameters.

For an interconnect circuit of more than two wires, the number of mutual inductance parameters is twice the number of different pairs of wires in the system. Since the latter is quadratic with the total number of wires, the overhead of calculating all mutual inductance parameters via coefficient

matching is enormous. For instance, 2 mutual inductance parameters are needed for 2 wires, 45 needed for 10 wires, and 4950 needed for 100 wires. However, it is not necessary to do so. When the distance between two wires is a few times, e.g., 3 times, larger than the largest cross section dimensions of both wires, the two mutual inductance parameters are very close to the low-frequency mutual inductance between the two wires. An example is provide in Section IV. In that case, one mutual inductance parameter will suffice to capture the proximity effect between two wires. That means only the mutual inductance parameters between a wire and its neighboring wires within some distance from this wire should be calculated via coefficient matching. Therefore, the total number of mutual inductance parameters needed to be calculated via coefficient matching as explained in this section is linear with the total number of wires in the interconnect circuit.

Although there are only two mutual inductance parameters between two reduced  $RL$  circuits, the number of mutual inductances can be much larger. Consider the general case as illustrated in Fig. 8. The worst case is when there are  $n_1 + n_2 - 1$  mutual inductances. However, this number can be reduced for many cases. As indicated by the simulation in Section IV, when the center distance between two wires is a few times, e.g., 3 times, larger than the largest cross section dimensions of both wires, the two mutual inductance parameters are very close to the low-frequency mutual inductance between the two wires. In this case, node voltages can be redefined when the two reduced  $RL$  circuits are decoupled, i.e., the number of mutual inductance reduces to zero. As an extension of this reduction technique, the two mutual inductance parameters between any two reduced  $RL$  circuits are compared against each other. Whenever the two parameters are close, the average is taken as the mutual inductance and the node voltages are redefined to get rid of  $n_1 + n_2 - 1$  mutual inductances. Another technique to reduce the number of mutual inductances is to calculate the coefficient of coupling. If a coefficient of coupling between some pair of inductors is very small, e.g., less than 0.02, then the mutual inductance is ignored.

A reduced  $RL$  circuit only contains a few branches. Furthermore, the number of a wire's close neighbors is much smaller than the total number of its neighbors. After applying the two reduction techniques explained above, it is expected that for an interconnect system, only a small portion of the matrices entries is nonzero in the state equations. Therefore, the overhead of applying the proposed skin and proximity effects model is low. Again, this is almost the minimal amount of extra circuit elements necessary to maintain high accuracy.

#### IV. SIMULATED DATA

When skin effect is negligible, to guarantee accurate simulation result, the interconnect wires are divided into smaller sections along its length using  $\pi$  or T sections. When skin effect is prominent, this approach is still needed and the skin effect model explained in Section II can be used to find the reduced  $RL$  circuit for each section of the wire. Consider three conductor sections all 1  $\mu\text{m}$  thick and 20  $\mu\text{m}$  long but 2-, 5-, and 10- $\mu\text{m}$  wide, respectively. Assume that the highest frequency of interest is 30 GHz and the conductivity takes the value  $3.5 \times 10^7$  S/m.

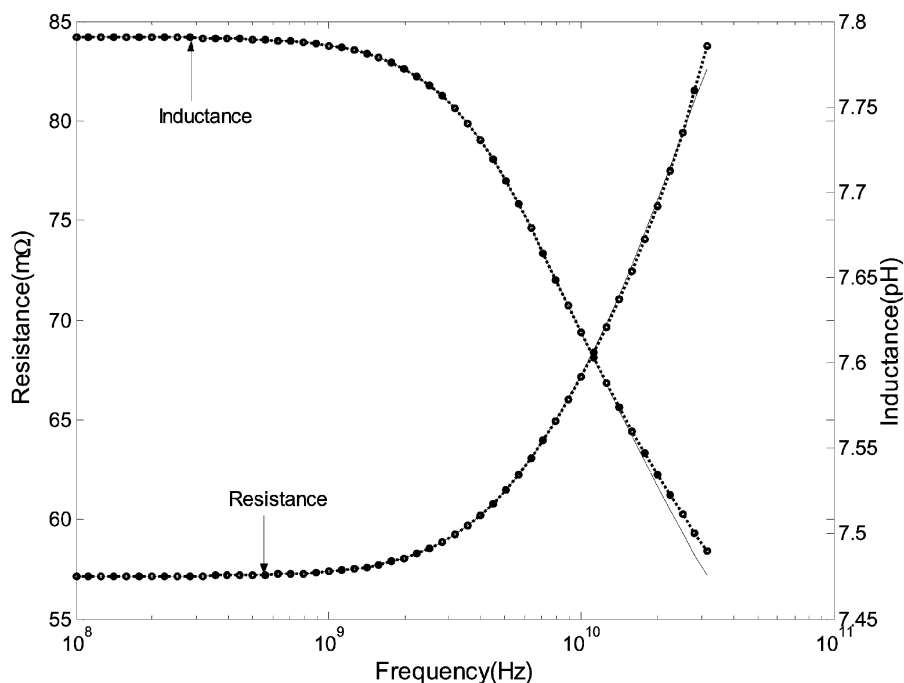


Fig. 9. Resistance and inductance calculated from the volume filament model and the three branches  $RL$  circuit for the  $10\ \mu\text{m}$  wide conductor.

TABLE II  
ACCURACY OF THE REDUCED  $RL$  CIRCUITS AS COMPARED TO THE  
VOLUME FILAMENT MODEL

Conductors of $1\ \mu\text{m}$ thick and $20\ \mu\text{m}$ long					
Width ( $\mu\text{m}$ )	# of $RL$ branches	Error boundary (%)			
		Resistance		Inductance	
		A	B	A	B
2	2	<b>0.0</b>	0.0	<b>0.0</b>	0.0
5	2	4.8	4.3	0.3	7.5
	3	<b>0.4</b>	1.9	<b>0.0</b>	1.9
10	2	15.4	6.6	0.2	20.7
	3	<b>1.4</b>	2.2	<b>0.1</b>	0.1

According to the skin depth formula  $\delta = \sqrt{1/(\pi\mu\sigma f)}$ , the skin depth at 30 GHz is  $0.49\ \mu\text{m}$ . To make the volume filament model accurate, the cross section of each conductor is divided into filaments of  $0.25 \times 0.25\ \mu\text{m}^2$ .

Properties of the reduced  $RL$  circuits shown in Fig. 9, Table I, and data A in Table II are obtained by matching leading coefficients in (11) and (12). Fig. 9 shows the resistance and inductance calculated from the volume filament model and the three branches  $RL$  circuit for the  $10\text{-}\mu\text{m}$  wide conductor. Dotted curves represent data calculated from the volume filament model while solid curves represent data calculated from the reduced  $RL$  circuits. This is also the case with the rest of the figures of  $R(f)L(f)$  curves. Table I shows the resistance and inductance in the reduced  $RL$  circuits. Data A in Table II indicate the maximum errors in the resistance and inductance in the frequency range of interest (up to 30 GHz) obtained from the volume filament model and the reduced  $RL$  model. As shown by data A in Table II, two branches give sufficient accuracy for the  $2\text{-}\mu\text{m}$  wire up to the frequency of interest (30 GHz). However, three branches are required for the  $5\ \mu\text{m}$  and  $10\ \mu\text{m}$  wires for an error of less than 1.4%.

Reduced  $RL$  circuits for those three wires are also obtained via matrix diagonalization and grouping technique explained in Section II. Impedances of these reduced  $RL$  circuits match those of the original circuits very well. Data B in Table II shows the maximum errors between the calculated resistance and inductance from the diagonalization and grouping technique and the original circuit, respectively, in the frequency range of interest up to 30 GHz.

The simulation reveals that the larger the cross section dimension of a wire, the more  $RL$  branches are needed to capture skin effect. This can be explained intuitively by recalling the skin depth formula  $\delta = \sqrt{1/(\pi\mu\sigma f)}$ . Apparently, resistances of wider and thicker conductors start to deviate from their dc values at lower frequency and increase with frequency. However, resistances of reduced  $RL$  circuits tend to saturate at high frequency, meaning that the  $RL$  branches that accurately capture skin effect impedance at low frequency are not accurate at high frequency. More  $RL$  branches are needed to improve the accuracy at high frequency. This trend means more  $RL$  sections are needed for conductors of bigger cross section dimensions.

In the submicrometer domain, the width and thickness of interconnect rarely exceed 40 and  $3\ \mu\text{m}$ , respectively. The proposed reduced  $RL$  circuit model was tested for interconnect wires of various cross section dimensions. The width was arbitrarily selected from the range  $(0, 40]\ \mu\text{m}$  and the thickness from the range  $(0, 3]\ \mu\text{m}$ . When six  $RL$  branches are used, in the frequency range from dc to 20 GHz, the maximum error between the resistance (or the inductance) from the proposed model and that from the volume filament model is 0.3%. In the frequency range from 20 to 30 GHz, the maximum error is 5% that corresponds to cross section dimensions  $3\ \mu\text{m} \times 40\ \mu\text{m}$  as shown in Fig. 2. Since the resistance and inductance in the whole frequency range of interest, e.g.,  $[0, 30\ \text{GHz}]$ , contribute to the time domain responses, the error in the time domain

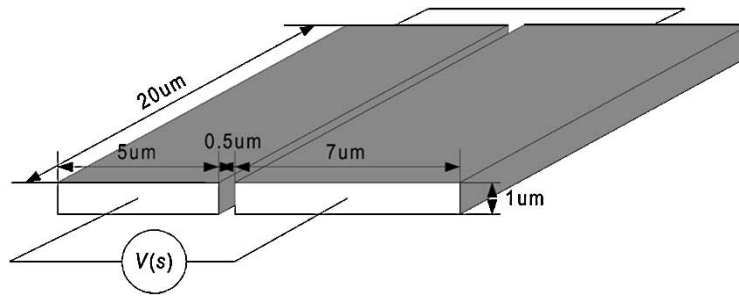
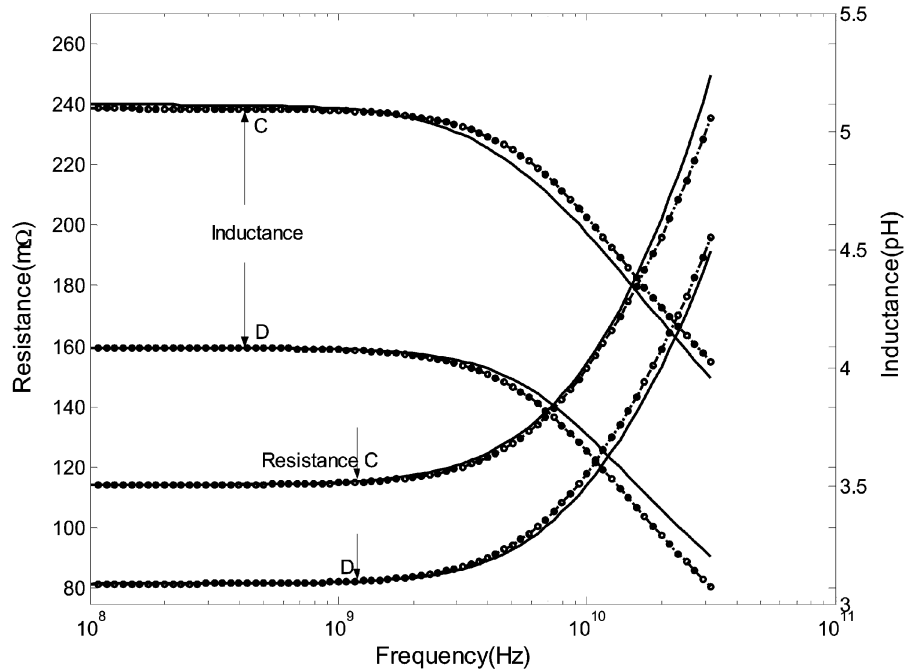


Fig. 10. Two wires connected in series .

Fig. 11. Resistance and inductance calculated from the volume filament model and the reduced  $RL$  circuit for the 5- and 7-  $\mu\text{m}$  conductors, respectively. Curves C's are for the 5-  $\mu\text{m}$  conductor while curves D's are for the 7  $\mu\text{m}$  conductor.

responses caused by the proposed model is much smaller than 5%.

As a guideline of using the proposed model to achieve good accuracy, it is suggested to use the reduced  $RL$  circuit to get 6 branches of resistance and inductance. To reduce the number of branches, the conductance of each of the six branches at the highest frequency of interest is calculated and those branches that contribute less than the allowed error number are removed from the reduced  $RL$  circuit. For example, if the maximum error between the resistance (or the inductance) from the reduced  $RL$  circuit and that from the volume filament model is set to be 1.5%, for a  $1\ \mu\text{m} \times 10\ \mu\text{m}$  interconnect wire, the number of branches in the reduced  $RL$  circuits shrinks from 6 to 3 as indicated by Fig. 9, Table I, and data A in Table II.

Fig. 10 shows the connection of two coplanar wires with currents flowing in opposite directions. The gap between the two wires is selected to be  $0.5\ \mu\text{m}$  to make the proximity effect prominent. Since the highest frequency of interest is selected to be 30 GHz and the penetration depth at this frequency is much smaller than the larger cross section dimensions of both wires, skin effect in both wires is prominent too. The skin and proximity model is applied to obtain the reduced  $RL$  circuit and the

TABLE III  
EXPANSION COEFFICIENTS

		5 $\mu\text{m}$ and 7 $\mu\text{m}$ wires		5 $\mu\text{m}$ and 10 $\mu\text{m}$ wires	
$M_1/M_0$		1.0		1.1	
$M_2/M_0$		4.9		3.9	
1 <sup>st</sup> ( $\times 10^{-10}$ )	From (14) and (15)	-5.2	-13.3	-6.5	23.8
	From (16) and (17)	-5.2	-13.3	-6.5	23.8
2 <sup>nd</sup> ( $\times 10^{-20}$ )	From (14) and (15)	10.0	17.8	14.5	37.7
	From (16) and (17)	10.0	17.8	14.3	37.9

mutual inductance parameters. The resistance and inductance of the 5  $\mu\text{m}$  and 7  $\mu\text{m}$  wires obtained from the reduced  $RL$  circuit are shown in Fig. 11 in comparison to those from the original  $RL$  circuit.

Table III shows the first and second order coefficients of the currents in (14)–(17) when expanded in powers of  $s$ . Two cases are considered. In case one, the 5- and 7- $\mu\text{m}$  wide wires are coplanar with center distance equal to  $6.5\ \mu\text{m}$ . In case two, the 5-

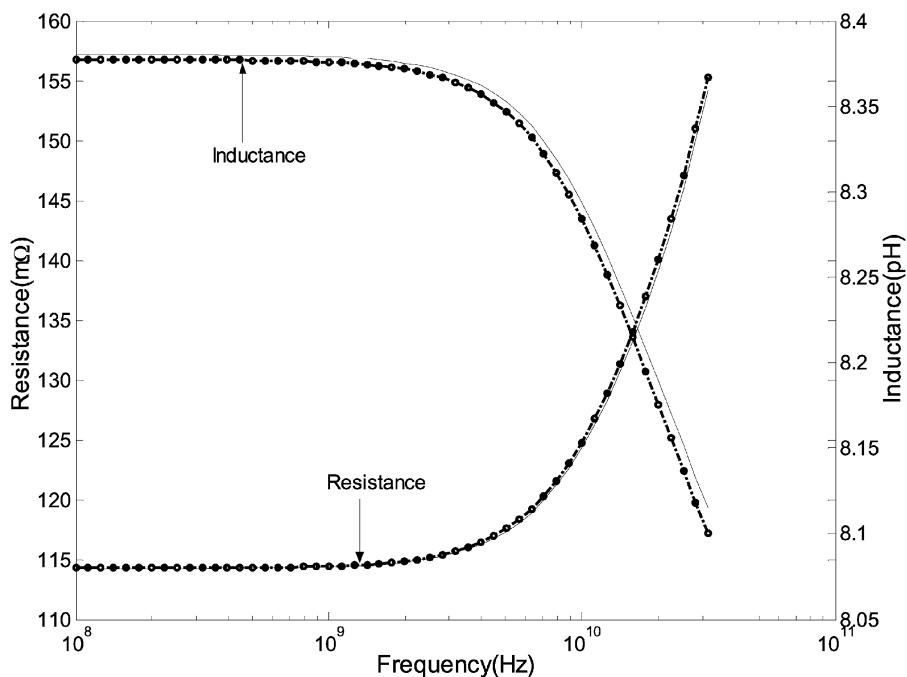


Fig. 12. Resistance and inductance calculated from the volume filament model and the reduced *RL* circuit for the 5  $\mu$ m conductor.

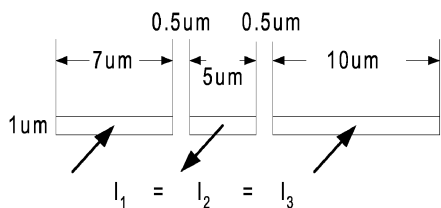


Fig. 13. Three coplanar wires all 20- $\mu$ m long with adjacent wires 0.5- $\mu$ m apart.

and 10- $\mu$ m wide wires are coplanar with center distance equal to 8  $\mu$ m.  $M_1/M_0$  and  $M_2/M_0$  represent the ratio of the two mutual inductance parameters with respect to the dc mutual inductance between the two wires. For each case, the two first order coefficients are calculated from (14) and (15) with arbitrary voltages  $V_1(s)$  and  $V_2(s)$ . Similarly, the two first-order coefficients are calculated from (16) and (17) with arbitrary voltages  $V_1(s)$  and  $V_2(s)$ . Second-order coefficients are calculated in the same manner. As can be seen, with appropriate mutual inductance parameters, for each case, the four pairs of coefficients match very well.

The same wires as in Fig. 10 are used to verify the claim in Section III that when the distance between two wires is a few times larger than the cross section dimensions of either wire, the two mutual inductance parameters are very close to the low-frequency mutual inductance between the two wires. The distance between the two center axes is selected to be 25  $\mu$ m. Since the two wire are coplanar, (3) is used to calculate the low-frequency mutual inductance between these two wires which is then assigned to the two mutual inductance parameters. The resistance and inductance of the 5  $\mu$ m wire obtained from the reduced *RL* circuit is shown in Fig. 12 in comparison to those from the original *RL* circuit.

Fig. 13 shows the connection of three coplanar wires all 20  $\mu$ m long and 1- $\mu$ m thick with gaps between adjacent wires equal to 0.5  $\mu$ m. The currents in the wires on two sides are

in the same direction and are opposite to the current in the middle wire. Again skin and proximity effects are prominent. The total width of the wires that carry the returning current is 17  $\mu$ m. Given the small gaps (0.5  $\mu$ m), this structure is expected to represent the worst case inductive coupling in the interconnect circuits in the leading VLSI design. The skin and proximity model is applied to obtain the reduced *RL* circuit elements and six mutual inductance parameters. The resistance and inductance of the 5- $\mu$ m wire calculated from the reduced *RL* circuits are shown in Fig. 14 in comparison to those from the original *RL* circuit. Programs written in Matlab are run on a PC with 2.4 GHz Pentium 4 CPU to obtain the curves shown in Fig. 14. It takes about 2 s to obtain all the resistance and self inductance values of the reduced *RL* circuit. Another 2 s is spent in obtaining mutual inductances between wires. With those parameters available, obtaining the curves for the reduced *RL* circuit only takes a fraction of one second. Thus, it takes less than 5 s in total to get those curves in Fig. 14 based on the reduced circuit model. In comparison, obtaining other curves in Fig. 14 based on the direct application of the volume filament model takes 127 s. Reduction of 96% of computation time is achieved. The reason is that the computation time saved due to substantial reduction in circuit size is much more than the overhead in calculating the reduced model. The reduction in computation for larger circuits is much greater.

Table IV shows the values of the mutual inductance parameters between the 5- and 7- $\mu$ m wires, those between the 5- and 10- $\mu$ m wires, and those between the 7- and 10- $\mu$ m wires in Fig. 13. These values are calculated by matching leading coefficients explained in Section III. The symbols  $M_{10}$ ,  $M_{20}$ , and  $M_{30}$  represent the low-frequency mutual inductance between the three pairs of wires calculated from (3).

To summarize, Fig. 9 and Tables I and II illustrate the accuracy of the skin effect model that is a special case of the skin and proximity effects model when the wire under consideration

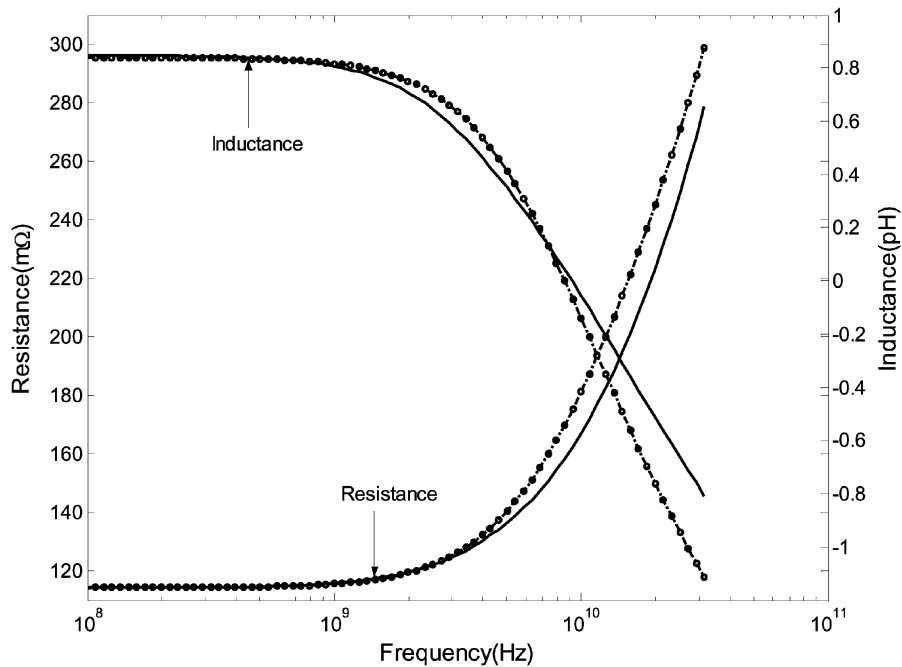


Fig. 14. Resistance and inductance calculated from the volume filament model and the reduced  $RL$  circuit for the  $5\text{-}\mu\text{m}$  conductor.

TABLE IV  
MUTUAL INDUCTANCE PARAMETERS BETWEEN WIRES TO CAPTURE  
PROXIMITY EFFECT

Between $5\ \mu\text{m}$ and $7\ \mu\text{m}$ wires	$1.058 \times M_{10}$	$M_{10} = 4.464\text{pH}$
	$2.89 \times M_{10}$	
Between $5\ \mu\text{m}$ and $10\ \mu\text{m}$ wires	$1.07 \times M_{20}$	$M_{20} = 3.881\text{pH}$
	$3.122 \times M_{20}$	
Between $7\ \mu\text{m}$ and $10\ \mu\text{m}$ wires	$1.04 \times M_{30}$	$M_{30} = 2.463\text{pH}$
	$1.2 \times M_{30}$	

is far away from other wires. Fig. 12 provides an evidence of showing the accuracy of the skin and proximity effects model when skin and proximity effects are prominent but proximity effect does not interact with skin effect. When skin effect, proximity effect, and the interaction between them are prominent, the skin and proximity effects model is shown to be valid and accurate by Figs. 11 and 14, and Table IV.

## V. CONCLUSION

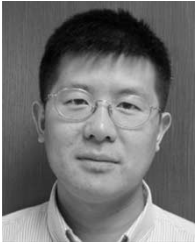
An efficient skin and proximity effects model is developed which accurately captures skin effect of wires by finding the reduced and decoupled  $RL$  circuits and captures proximity effect by finding mutual inductance parameters between reduced and decoupled  $RL$  circuits of wires. This model is realizable and guarantees high accuracy at six branches of resistance and inductance in the frequency range of interest for interconnect wires with thickness up to  $3\ \mu\text{m}$  and width up to  $40\ \mu\text{m}$ . Some  $RL$  branches can be removed depending on the permitted error number. If the cross section of a wire is divided into identical filaments, then only simple matrix multiplication and simple arithmetic are needed to calculate resistance and inductance of the reduced and decoupled  $RL$  circuit of the wire. Similarly, only the inversion of diagonal resistance matrix, simple matrix multipli-

cation, and simple arithmetic are needed in calculating mutual inductance parameters between two reduced and decoupled  $RL$  circuits of a pair of wires. Furthermore, the number of mutual inductance parameters needed to be calculated via matrix multiplication, etc., is linear with the number of wires.

## REFERENCES

- [1] S. Mei, C. Amin, and Y. I. Ismail, "Efficient model order reduction including skin effect," *Proc. Design Automation Conf.*, pp. 232–237, June 2003.
- [2] Y. Cao, X. Huang, D. Sylvester, T. King, and C. Hu, "Impact of on-chip interconnect frequency-dependent  $R(f)L(f)$  on digital and RF design," in *Proc. ASIC/SOC Conf.*, 2002, pp. 438–442.
- [3] K. M. Coperich and A. E. Ruehli, "Enhanced skin effect for partial-element equivalent-circuit (PEEC) models," *IEEE Trans. Microwave Theory Tech.*, vol. 48, pp. 1435–1442, Sept. 2000.
- [4] M. Xu and L. He, "An efficient model for frequency-dependent on-chip inductance," in *Proc. 2001 Conf. Great Lakes Symp. VLSI*, 2001, pp. 115–120.
- [5] M. J. Tsuk and A. J. Kong, "A hybrid method for the calculation of the resistance and inductance of transmission lines with arbitrary cross sections," *IEEE Trans. Microwave Theory Tech.*, vol. 39, pp. 1338–1347, Aug. 1991.
- [6] L. Daniel, A. Sangiovanni-Vincentelli, and J. White, "Using conduction modes basis functions for efficient electromagnetic analysis of on-chip and off-chip interconnect," *Proc. Design Automation Conf.*, pp. 563–566, June 2001.
- [7] L. T. Pillage and R. A. Rohrer, "Asymptotic waveform evaluation for timing analysis," *IEEE Trans. Computer-Aided Design*, vol. 9, pp. 352–366, Apr. 1990.
- [8] P. Silvester, "Modal network theory of skin effect in flat conductors," in *Proc. IEEE*, vol. 54, 1966, pp. 1147–1151.
- [9] H. A. Wheeler, "Formulas for the skin effect," in *Proc. Inst. Radio Eng.*, vol. 30, 1942, pp. 412–424.
- [10] S. Kim and D. P. Neikirk, "Compact equivalent circuit model for the skin effect," in *Proc. 1996 IEEE Int. Microwave Symp.*, San Francisco, CA, June 1996.
- [11] M. F. Caggiano, E. Barkley, M. Sun, and J. T. Kleban, "Electrical modeling of the chip scale ball grid array package at radio frequencies," *Microwaves J.*, vol. 31, pp. 701–709, 2000.
- [12] B. Krauter and S. Mehrotra, "Layout based frequency dependent inductance and resistance extraction for on-chip interconnect timing analysis," in *Proc. 35th Annu. Conf. Design Automation*, 1998, pp. 303–308.

- [13] B. E. Keiser, *Principles of Electromagnetic Compatibility*. Norwood, MA: Artech House, 1979, p. 102.
- [14] E. B. Rosa, "The self and mutual inductance of linear conductors," *Bulletin Nat. Bureau Standards*, vol. 4, pp. 301–344, 1908.
- [15] M. Kamon, N. Marques, L. M. Silveira, and J. White, "Generating reduced order models via PEEC for capturing skin and proximity effects," in *Proc. 6th Tropical Electrical Performance of Electronic Packaging*, San Jose, CA, 1997, pp. 259–262.



**Shizhong Mei** received the B.S. degree in physics from University of Science and Technology of China, Hefei, Anhui, in 1994, the M.S. degree in physics from Beijing University, Beijing, China, in 1998, and the M.S. degree in electrical engineering Northwestern University, Evanston, IL, in 2001, where he is currently working toward the Ph.D. degree in electrical engineering.

In 2001, he was with Charles Industries Company, Rolling Meadow, IL, as a field-programmable gate arrays FPGA designer. In summer 2003, he was with Synopsys, Mountain View, CA, where he was engaged in structured ASIC design and gate delay modeling research. His research interests include high-speed interconnect modeling, gate modeling, timing analysis, and VLSI design.



**Yehea I. Ismail** (M'00) was born in Giza, Egypt on November 11, 1971. He received the B.Sc. and M.S. degree in electronics and communications engineering with distinction and honors from Cairo University, Cairo, Egypt, in 1993 and 1996, respectively, the Masters and the Ph.D. degrees from the University of Rochester, Rochester, NY, in 1998 and 2000, respectively.

In August 1993, as one of the top of his class, he was appointed as a Teacher Assistant, in the Department of Electrical and Computer Engineering, Cairo University. He is currently with Northwestern University, Evanston, IL, as an Assistant Professor. He was with IBM Cairo Scientific Center (CSC), from 1993 to 1996, and with IBM Microelectronics, Fishkill, NY, from 1997 to 1999. He has authored more than 50 technical papers and a book. His primary research interests include interconnect, noise, innovative circuit simulation, and related circuit level issues in high-performance VLSI circuits.

Prof. Ismail is on the Editorial Board of the IEEE TRANSACTIONS ON VERY LARGE SCALE INTEGRATION (VLSI) SYSTEMS, on the Editorial Board of the IEEE TRANSACTIONS ON CIRCUITS AND SYSTEMS I: FUNDAMENTAL THEORY AND APPLICATIONS, and a Guest Editor for a special issue of the IEEE TRANSACTIONS ON VERY LARGE SCALE INTEGRATION (VLSI) SYSTEMS on "On-Chip Inductance in High Speed Integrated Circuits." He was selected as the 2002 IEEE Circuits and Systems Society Outstanding Young Author Award Winner. He also won the National Science Foundation Career Award in 2002. He was given the Best Teacher Award from the Electrical and Computer Engineering Department, Northwestern University, Evanston, IL, in 2003.